

ELLIPTIC FLOW OF STRANGE AND MULTI-STRANGE PARTICLES IN Pb–Pb COLLISIONS AT $\sqrt{s_{NN}} = 2.76$ TeV MEASURED WITH ALICE*

ZHONG-BAO YIN

for the ALICE Collaboration

Key Laboratory of Quarks and Lepton Physics (MOE)

and

Institute of Particle Physics, Central China Normal University

Wuhan 430079, China

(Received January 25, 2013)

Measurement by ALICE of the elliptic flow coefficient (v_2) of strange and multi-strange particles (K_S^0 , K^\pm , Λ , Ξ , Ω , ϕ) as a function of transverse momentum, p_T are compared with those of charged pions and (anti-) protons measured at mid-rapidity in Pb–Pb collisions at $\sqrt{s_{NN}} = 2.76$ TeV. The mass splitting and the constituent quark number (n_q) scaling of v_2 are studied as a function of collision centrality. v_2/n_q versus p_T/n_q scales within 20% for all identified particles for $p_T/n_q \sim 1.2$ GeV/c, while n_q scaling of v_2 in transverse kinetic energy ($m_T - m_0$) is broken over the low $(m_T - m_0)/n_q$ region. The p_T differential v_2 values are compared to the viscous hydrodynamical (VISH2+1) model calculation and to the STAR measurements in Au–Au collisions at $\sqrt{s_{NN}} = 200$ GeV. The model calculations can reproduce the main features of identified particle v_2 at low p_T . The differential flow of ϕ indicates a larger radial flow at LHC than that at RHIC, while the flow of Ξ and Ω is similar to that measured by STAR for Au–Au collisions at $\sqrt{s_{NN}} = 200$ GeV.

DOI:10.5506/APhysPolBSupp.6.479

PACS numbers: 25.75.Dw, 25.75.Gz, 25.75.Ld, 21.65.Qr

1. Introduction

Interactions among medium constituents in heavy-ion collisions transform the initial spatial anisotropy into the final momentum anisotropy of observed particles. The momentum anisotropy can be characterized by the v_n coefficients of the Fourier expansion of the particle azimuthal distribution relative to the reaction plane [1]. The second coefficient, v_2 , usually

* Presented at the International Symposium on Multiparticle Dynamics, Kielce, Poland, September 17–21, 2012.

called the elliptic flow parameter, is related to eccentricity of initial spatial anisotropy, while odd and higher order harmonics at mid-rapidity are induced by fluctuations in the initial shape of the interaction region [2]. Elliptic flow of identified particles measured as a function of transverse momenta, p_T , is among the most informative observables for understanding the dynamics of the collisions and the fundamental properties of the created quark matter [3]. At low p_T , the species dependence of v_2 , which is well described by hydrodynamics, is sensitive to the transport properties of the medium created in heavy-ion collisions. At intermediate p_T of $\sim 3\text{--}6$ GeV/ c , the constituent quark number (n_q) scaling may reflect the details of early partonic dynamics and hadronization mechanism. However, since azimuthal anisotropy develops through the whole collision evolution, both partonic and hadronic stages may contribute to the observed transverse flow. To estimate the relative contributions to the elliptic flow from early deconfined partonic interactions and later hadronic rescatterings in the system evolution, it is useful to measure the elliptic flow of multi-strange particles. Multi-strange particles have small hadronic cross-sections [4, 5] and, therefore, are expected to be mainly sensitive to the quark-gluon-plasma phase.

In this contribution, we present v_2 as a function of p_T for strange and multi-strange particles (K_S^0 , K^\pm , ϕ , Λ , Ξ and Ω) and compare it to that of charged pions and (anti-)protons measured in Pb–Pb collisions at $\sqrt{s_{NN}} = 2.76$ TeV with the ALICE detector. Results are compared to the hydrodynamical model calculations and RHIC measurements in Au–Au collisions at $\sqrt{s_{NN}} = 200$ GeV [6].

2. Data analysis

This analysis is based on a sample of about 10 million minimum bias Pb–Pb collisions at $\sqrt{s_{NN}} = 2.76$ TeV recorded with ALICE during the 2010 LHC running. The standard ALICE minimum bias event selection criteria [7] for Pb–Pb collisions were applied. Only events with a reconstructed vertex at $|v_z| < 10$ cm along the beam axis were used. The event centrality was determined based on the sum of the amplitudes measured in the VZERO detectors [8]. Charged pions, kaons, and protons were reconstructed using the ITS and TPC detectors. Tracks were selected in the pseudo-rapidity range $|\eta| < 0.8$. Strange and multi-strange particles were reconstructed via their weak decay channels: $K_S^0 \rightarrow \pi^+\pi^-$, $\Lambda \rightarrow p + \pi^-$ ($\bar{\Lambda} \rightarrow \bar{p} + \pi^+$), $\phi \rightarrow K^+K^-$, $\Xi^- \rightarrow \Lambda + \pi^-$ ($\bar{\Xi}^+ \rightarrow \bar{\Lambda} + \pi^+$) and $\Omega^- \rightarrow \Lambda + K^-$ ($\bar{\Omega}^+ \rightarrow \bar{\Lambda} + K^+$). Combinatorial background in K_S^0 , Λ , Ξ and Ω measurements was reduced by applying cuts selecting specific decay topologies and using information on the specific energy loss in TPC of their decay daughters. In the case of ϕ meson, the combinatorial background was suppressed by combining the information on the decay daughters' energy loss in TPC and their time-of-flight in the TOF detectors.

The elliptic flow parameter v_2 was measured using two-particle, scalar product, and event plane methods [9]. The event plane angle and the flow vector were determined from charged particles reconstructed with TPC and from azimuthal distribution of hits in forward VZERO detectors. Charged pions, kaons and protons were selected in the range $|\eta| < 0.8$, while strange and multi-strange candidates in $|\eta| < 0.5$. Contribution from elliptic flow of the combinatorial background pairs, v_2^{bg} , in the (multi-)strange particles v_2 measurement was removed by studying the azimuthal correlations *versus* pair invariant mass, m_{inv} (either invariant mass side band or v_2 *versus* m_{inv} method [10]). Since v_2 is additive, candidate v_2^{tot} *versus* pair invariant mass can be expressed as a sum of signal v_2^{sig} and background v_2^{bg} weighted by their relative yields

$$v_2^{\text{tot}}(m_{\text{inv}}) = v_2^{\text{sig}} \frac{N^{\text{sig}}}{N^{\text{tot}}}(m_{\text{inv}}) + v_2^{\text{bg}}(m_{\text{inv}}) \frac{N^{\text{bg}}}{N^{\text{tot}}}(m_{\text{inv}}), \quad (1)$$

where N^{tot} is the total number of candidates, N^{bg} and $N^{\text{sig}} = N^{\text{tot}} - N^{\text{bg}}$ are the number of signal and background pairs for a given invariant mass bin and p_{T} bin. In the invariant mass side band method, v_2^{tot} and v_2^{bg} are determined from the signal mass band and two mass side-bands of the signal region, respectively. In the v_2 *versus* invariant mass method, v_2^{sig} is extracted by a combined (simultaneous) fit of the invariant mass distribution and $v_2(m_{\text{inv}})$ using Eq. (1).

3. Results

Figure 1 shows v_2 of K_{S}^0 , $\Lambda(\bar{\Lambda})$ and ϕ v_2 along with that of charged pion, kaon and (anti-)proton [11]. A clear mass ordering of v_2 is observed for $p_{\text{T}} < 2.5$ GeV/ c with v_2 of heavier hadrons to be smaller than that of light particles. The relative mass-splitting of v_2 increases with centrality. This can be explained by the stronger axially symmetric radial flow [12] for more central heavy-ion collisions to shift the elliptic flow to larger p_{T} for heavier particles. At low p_{T} , the ϕ -meson elliptic flow is similar to that of (anti-)proton, indicating a similar radial flow effect on particles of similar mass. As shown in the left panel of Fig. 2, the main features of the mass dependence of v_2 including that of multi-strange baryons are reproduced by viscous hydrodynamic model (VISH2+1) calculations [13]. A better agreement is observed in the right panel of Fig. 2 for the 40–50% central collisions. For central collisions, viscous hydrodynamic calculations fail to reproduce the proton and ϕ v_2 , which may indicate an additional build-up of v_2 due to rescatterings in the hadronic phase [13].

In the intermediate p_{T} region, v_2/n_q *versus* p_{T}/n_q scaling serves as a test of the hadron production via quark coalescence. The transverse kinetic energy $(m_{\text{T}} - m_0)/n_q$ scaling, which was observed in the low p_{T} region at

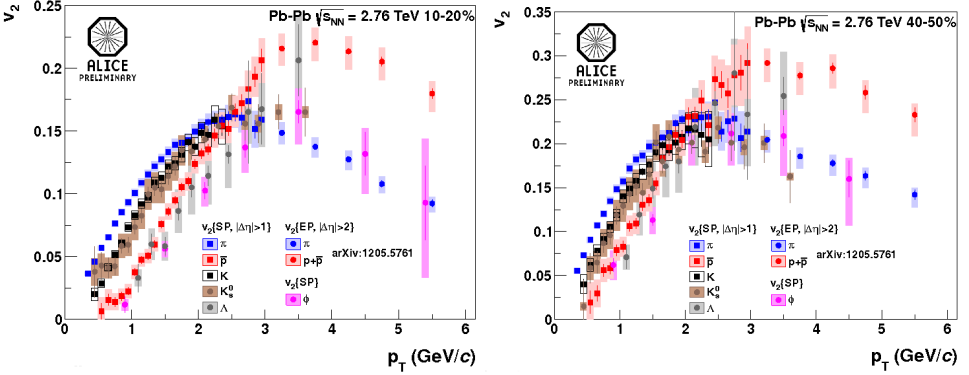


Fig. 1. K_S^0 , $\Lambda(\bar{\Lambda})$ and ϕ v_2 compared with charged pion, kaon and (anti-)proton v_2 measured for 10–20% (left) and 40–50% (right) central Pb–Pb collisions at $\sqrt{s_{NN}} = 2.76$ TeV.

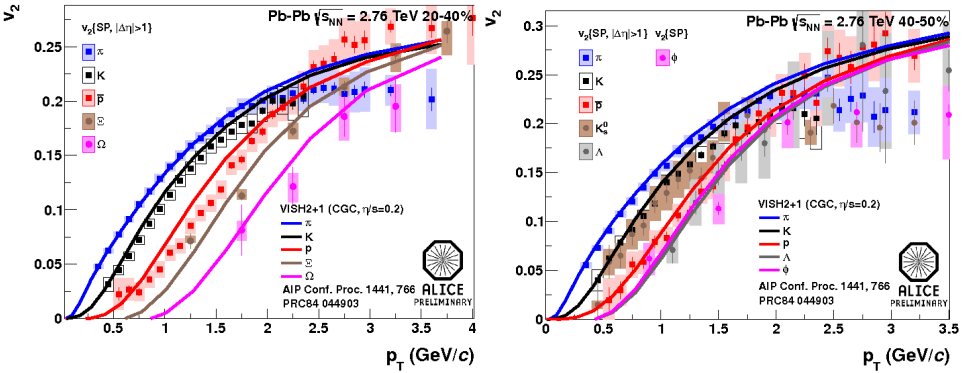


Fig. 2. v_2 as a function of p_T for identified particles in Pb–Pb collisions at 2.76 TeV compared to viscous hydrodynamic model calculations [13] for 20–40% centrality focusing on Ξ and Ω flow (left) and for 10–20% centrality focusing on ϕ flow (right).

the top RHIC energy [14], is aimed to compensate the mass dependence of v_2 which originates from the hydrodynamic radial expansion of the system. The n_q scaling is tested for various centrality bins in Pb–Pb collisions at $\sqrt{s_{NN}} = 2.76$ TeV. Figure 3 shows v_2 in 10–20% centrality class scaled by n_q as a function of p_T/n_q (left) and as a function of $(m_T - m_0)/n_q$ (right), where $m_T = \sqrt{p_T^2 + m_0^2}$ and m_0 is the particle mass. The n_q scaling of the identified particle v_2 versus p_T/n_q at the LHC holds approximately within 20% at $p_T/n_q \sim 1.2$ GeV/c, while the transverse kinetic energy n_q scaling of elliptic flow is not observed over the low $(m_T - m_0)/n_q$ region.

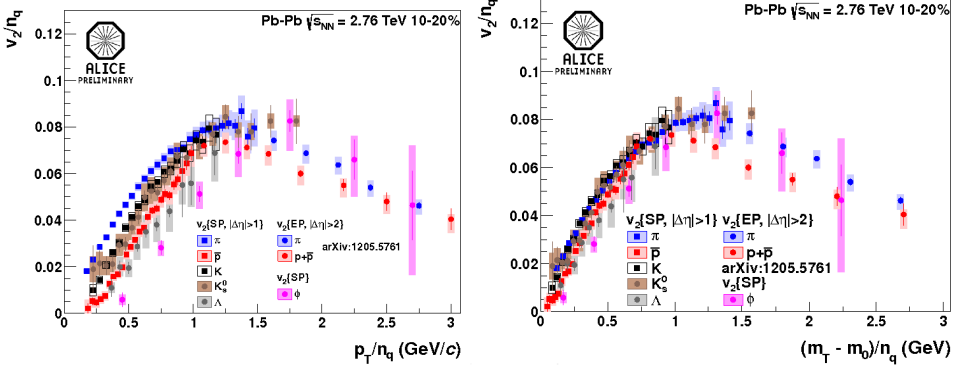


Fig. 3. v_2 scaled by n_q as a function of p_T/n_q (left) and $(m_T - m_0)/n_q$ (right).

Compared with the STAR measurements [6] as shown in Fig. 4, ϕ -meson v_2 indicates larger radial flow at the LHC as observed already from v_2 and spectra of charged pion, kaon and proton [15]. The p_T differential v_2 of multi-strange baryons is similar to that measured at RHIC energy. This might indicate that multi-strange baryons are less affected by the hadronic phase of the collision evolution.

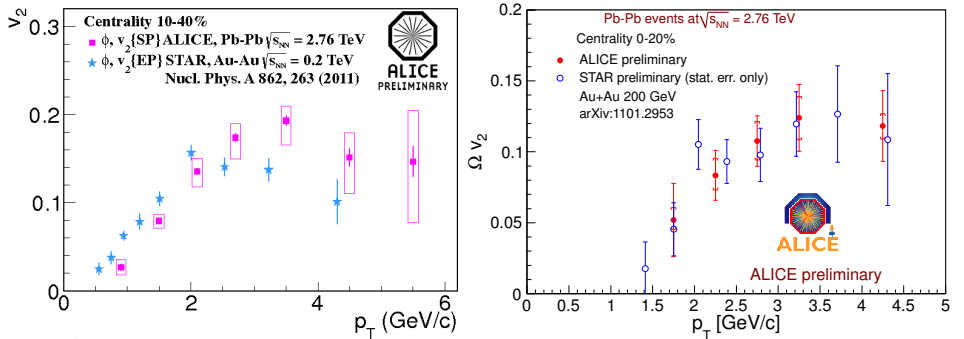


Fig. 4. Comparison of ϕ v_2 (left) for 10–40% centrality and $\Omega^- + \bar{\Omega}^+$ v_2 (right) for 0–20% centrality in Pb–Pb collisions at $\sqrt{s_{NN}} = 2.76$ TeV to the STAR measurements in Au–Au collisions at $\sqrt{s_{NN}} = 200$ GeV.

4. Summary

ALICE presented the elliptic flow parameter of strange and multi-strange particles compared with that of charged pions and (anti-)protons measured at mid-rapidity in Pb–Pb collisions at $\sqrt{s_{NN}} = 2.76$ TeV. The mass ordering of the elliptic flow, which is observed for all measured species at low p_T , is qualitatively reproduced by viscous hydrodynamic model calcu-

lations. v_2/n_q versus p_T/n_q scales within 20% for all identified species at $p_T/n_q \sim 1.2$ GeV/ c , while the transverse kinetic energy n_q scaling of v_2 is broken over the low $(m_T - m_0)/n_q$ region. The differential flow of ϕ indicates also a larger radial flow at LHC than at RHIC, while the differential flow of Ξ and Ω is similar to the STAR measurements in Au–Au collisions at $\sqrt{s_{NN}} = 200$ GeV.

This work is supported partly by the National Natural Science Foundation of China (NSFC) under grants Nos. 10975061 and 11020101060.

REFERENCES

- [1] A.M. Poskanzer, S.A. Voloshin, *Phys. Rev.* **C58**, 1671 (1998).
- [2] B. Elvera, G. Roland, *Phys. Rev.* **C81**, 054905 (2010) [*Erratum ibid.* **C82**, 039903 (2010)].
- [3] R. Snellings, *New J. Phys.* **13**, 055008 (2011).
- [4] A. Shor, *Phys. Rev. Lett.* **54**, 1122 (1985).
- [5] H. van Hecke, H. Sorge, N. Xu, *Phys. Rev. Lett.* **81**, 5764 (1998).
- [6] S. Shi [STAR Collaboration], *Nucl. Phys.* **A862**, 263c (2011).
- [7] K. Aamodt *et al.* [ALICE Collaboration], *Phys. Lett.* **B696**, 30 (2011).
- [8] K. Aamodt *et al.* [ALICE Collaboration], *Phys. Rev. Lett.* **105**, 252301 (2010).
- [9] C. Adler *et al.* [STAR Collaboration], *Phys. Rev.* **C66**, 034904 (2002).
- [10] N. Borghini, J.Y. Ollitrault, *Phys. Rev.* **C70**, 064905 (2004).
- [11] M. Krzewicki [ALICE Collaboration], *J. Phys. G* **38**, 124047 (2011).
- [12] N. Herrmann, J.P. Wessels, T. Wienold, *Annu. Rev. Nucl. Part. Sci.* **49**, 581 (1999).
- [13] U.W. Heinz, C. Shen, H. Song, *AIP Conf. Proc.* **1441**, 766 (2012).
- [14] A. Adare *et al.* [PHENIX Collaboration], *Phys. Rev. Lett.* **98**, 162301 (2007).
- [15] B. Abelev *et al.* [ALICE Collaboration], *Phys. Rev. Lett.* **109**, 252301 (2012).